PROSPECTS
IN PHARMACEUTICAL SCIENCES

Prospects in Pharmaceutical Sciences, 24(1), 1-16
https://prospects.wum.edu.pl/

Original Article

DEVELOPMENT AND OPTIMIZATION OF GASTRO RETENTIVE FLOATING TABLETS OF DAPSONE FOR CONTROLLED RELEASE

Rushikesh Mahale*[1†], Shivraj Jadhav[1†], Sunil Mahajan[2]

[1]*Department of Pharmaceutics, Shreeshakti Shaikshanik Sanstha's Divine College of Pharmacy, Nampur Road, Satana, Nashik, Maharashtra, India -423301*

[2]*Department of Pharmaceutical Chemistry, Shreeshakti Shaikshanik Sanstha's Divine College of Pharmacy, Nampur Road, Satana, Nashik, Maharashtra, India -423301*

* Correspondence, e-mail: rushikeshkailasmahale@gmail.com

Received: 08.06.2025 / Revised: 16.08.2025 / Accepted: 16.08.2025 / Published online: 01.09.2025 / Published in final version: 08.01.2026

ABSTRACT

The objective of this study was to develop and optimize gastroretentive floating tablets of dapsone using a Quality by Design approach to enhance therapeutic efficacy in leprosy treatment. The tablets were prepared by direct compression using a 3^2 factorial design, with HPMC K15M (150—250 mg) and $NaHCO_3$ (15—25 mg) as independent variables. The formulations were evaluated for compression parameters, floating characteristics, and drug release profiles, with optimization focused on floating lag time (Y1) and drug release at 12 hours (Y2) as key responses. Further studies assessed release kinetics, formulation stability, and a comparison with a marketed product. The optimized formulation (RF3), composed of 150 mg HPMC K15M and 25 mg $NaHCO_3$, exhibited excellent flow properties (Carr's index: 15.25%, angle of repose: 26.84°), desirable floating behavior (lag time: 64 seconds, duration: 11.4 hours), and sustained drug release (98.4% over 12 hours). The drug release followed the Higuchi model (R^2 = 0.9975) with a non-Fickian transport mechanism (n = 0.75). Stability studies under accelerated conditions (40 °C/75% RH for 6 months) confirmed drug content retention of 98.24% and a consistent release profile (97.4% at 12 hours). Overall, the optimized gastroretentive floating tablet formulation demonstrated satisfactory in vitro performance and stability, suggesting promising advantages over conventional dosage forms through extended gastric retention and controlled drug release. While these findings support the potential of this novel formulation for modified dapsone delivery, comprehensive in vivo studies are necessary to validate its therapeutic benefits over existing therapies.

KEYWORDS: dapsone, gastroretentive drug delivery, floating tablets, quality by design.

1. Introduction

Leprosy remains a significant global health concern, with over 200,000 newly detected cases annually, predominantly in developing regions of Asia, Africa, and South America. Dapsone, a key component of multidrug therapy (MDT), faces several limitations when administered orally in tablet form. However, conventional dapsone tablets are associated with multiple pharmacokinetic and tolerability issues, contributing to reduced treatment effectiveness and patient adherence [1]. Additionally, leprosy imposes significant economic burdens, with estimated costs ranging from $100 to $150 million annually. These include direct treatment expenses, productivity losses, and expenditures related to social rehabilitation [2]. Standard regimens that mandate dapsone use often result in substantial fluctuations in plasma drug levels throughout the day, potentially increasing the risk of toxicity. Moreover, delayed diagnosis and irregular treatment adherence, particularly in areas with limited healthcare access, continue to drive disease transmission in endemic regions [3].

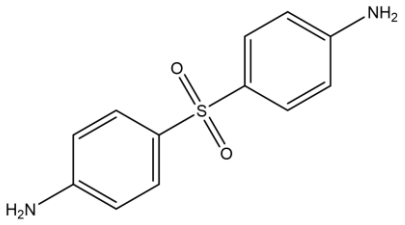

Fig. 1. Chemical structure of dapsone

Dapsone (4,4-diaminodiphenyl sulfone), shown in Fig. 1, is one of the oldest and most effective antibiotics used in leprosy treatment, having been widely adopted since the launch of leprosy control programs in 1946 [3]. It is a synthetic sulfone with bacteriostatic activity,

a molecular weight of 248.3 Da, and a log P value of 0.97. Published data indicate an oral absorption rate of 70—85% and an elimination half-life of 20—30 hours [4]. In addition to its antimicrobial effects, dapsone also exhibits anti-inflammatory activity, making it useful in other dermatological conditions. However, modern formulation science has revealed challenges in the physicochemical stability of dapsone, necessitating improved drug delivery strategies [5].

Gastroretentive drug delivery systems (GRDDS) have emerged as an innovative approach to improve drug bioavailability and therapeutic efficacy. These systems utilize hydrophilic polymers and gas-generating agents to enable the dosage form to float in the stomach for prolonged periods, thus enhancing gastric retention and enabling sustained drug release. This strategy addresses limitations in traditional formulations, such as erratic drug release, high dosing frequency, and suboptimal bioavailability [6].

Despite the extensive research on gastroretentive systems, dapsone has not been previously formulated as a gastroretentive floating tablet using a Quality by Design approach. Current dapsone therapy in leprosy treatment faces significant challenges, including poor aqueous solubility, gastrointestinal irritation, variable bioavailability, peak-related side effects, and poor patient compliance, particularly in resource-limited settings where leprosy is endemic [7]. While gastroretentive systems have been developed for various drugs, the specific combination of dapsone's physicochemical properties (molecular weight 248.3 Da, log P 0.97, half-life 28 hours) with an HPMC K15M matrix has not been systematically optimized for sustained gastric retention. The novelty of this work lies in: (1) the first application of QbD methodology to dapsone gastroretentive formulation, (2) the systematic optimization of the HPMC K15M-$NaHCO_3$ combination specifically for dapsone's unique properties, (3) the development of a sustained-release system designed to deliver the drug over 12 hours, aiming to maintain consistent plasma levels and improve therapeutic efficacy in leprosy management, and (4) the development of a GRDDS for dapsone that is scientifically justified, not for extending dosing intervals, but for optimizing its therapeutic performance and minimizing dose-dependent toxicity. The rapid progress in polymer science has ensured that the matrices in use can be designed to have structural stability as well as the ability to deliver the drug over 12—24 hours. The floating tablets showed enhanced stability in gastric condition compared with the regular formulations and in vitro studies proved that the drug release characteristics and the floating time exceeded 12 hours [8].

The objective of the present work is to design and evaluate gastroretentive floating tablets containing dapsone for the improved management of leprosy. This would involve determining the floating characteristics and drug release profile, assessing the effects of formulation factors on the performance of the tablets, and the biopharmaceutical evaluation and setting up of the in vitro correlation. This research aims to develop strategies for enhancing dapsone therapy, where existing challenges are addressed, especially regarding formulation, without compromising cost and scalability.

2. Materials and Methods

2.1. Materials

Dapsone (USP grade, 99.9% purity) was procured from Sciquaint Innovations Private Limited (Pune, India). Hydroxypropyl methylcellulose (HPMC K15M, pharmaceutical grade) and sodium bicarbonate ($NaHCO_3$, analytical grade, 99.5% purity) were obtained from Research Lab Fine Chem Industries (Mumbai, India). Polyvinylpyrrolidone (PVP K30, pharmaceutical grade) and magnesium stearate (USP grade) were sourced from Merck Limited (Mumbai, India). Microcrystalline cellulose (MCC PH102, pharmaceutical grade) and talc (USP grade) were purchased from Sciquaint Chemicals (Pune, India). All other chemicals and reagents used in the study were of analytical grade and used as received without further purification.

2.2. Methods

2.2.1. Calibration Curve of Dapsone

Ethanol was selected as the solvent for determining dapsone spectral characteristics due to its better solubility and stability compared to acidic media. A total of 10 mg of pure dapsone was accurately weighed and transferred to a 100 mL (100 µg/mL) volumetric flask, dissolved with ethanol, and made up to the mark. 1.0% ethanol in sterile water was used for preparing the stock solution of dapsone at a concentration of 100 µg/mL. Using the prepared stock solution of 100 µg/mL, a dilution procedure was performed by withdrawing different volumes (0.5, 1.0, 1.5, 2.0, 2.5, 3.0 mL) of the standard solution, transferred into six sets of 10 mL volumetric flasks, and then made up to volume with ethanol, which led to the preparation of working standard solutions containing concentrations ranging from 5 to 30 µg/mL. The absorbance of each solution was measured at λmax of 293 nm using a Shimadzu UV-1800 spectrophotometer, as per literature standards [9]. The UV spectrophotometric method was validated according to ICH Q2 (R1) guidelines. Linearity was established with a coefficient of determination (r^2) of 0.9971 across the concentration range of 5—30 µg/mL. Precision studies showed a relative standard deviation (RSD) < 2% for both intraday and interday measurements (n = 6). Accuracy was determined by recovery studies at 80%, 100%, and 120% levels, showing a mean recovery of 98.5—101.2%. The method demonstrated specificity with no interference from excipients at the analytical wavelength.

2.2.2. Fourier Transform Infrared (FTIR) Spectroscopy

Fourier Transform Infrared Spectroscopy (FTIR) studies were conducted using a Perkin Elmer Paragon 1000 FTIR spectrometer equipped with an attenuated total reflectance (ATR) accessory. Samples of pure dapsone and the optimized formulation were measured in the range of 4000 to 400 cm^{-1} at a resolution of 4 cm^{-1} with 32 cumulative scans. The samples were deposited directly onto the ATR crystal and analyzed at an ambient temperature of 25 ± 2 °C. The obtained spectra were evaluated for characteristic absorption frequencies to identify any possible physical interactions between the drug and excipients [10,11].

2.2.3. Differential Scanning Calorimetry (DSC)

Differential Scanning Calorimetry analysis was performed using a Shimadzu DSC-60 thermal analyser (Japan). Pure dapsone ranging from 5—8 mg was weighed, placed in aluminium pans, and subsequently mixed with appropriate samples as well as physical mixtures. The samples were heated starting from 25 °C up to 300 °C with a scanning rate of 10°C/min, with a nitrogen gas flow rate of 50 mL/min. A reference material in the form of an empty aluminium pan was also used. Thermal studies were conducted by DSC in order to determine thermal properties and possible incompatibilities in terms of peak temperature, onset temperature, and enthalpy changes (ΔH) [12,13].

2.2.4. QbD Approach for Formulation Design

The formulation optimization was performed using a Quality by Design (QbD) approach employing a 3^2 full factorial design. Two independent variables were selected: X_1 (HPMC K15M concentration, 150—250 mg) and X_2 ($NaHCO_3$ concentration, 15—25 mg), each evaluated at three levels coded as -1 (low), 0 (medium), and +1 (high). The dependent variables (responses) studied were Y_1 (floating lag time in seconds) and Y_2 (percentage drug release at 12 hours). Design-Expert® software (Version 12, Stat-Ease Inc., Minneapolis, USA) was used for the experimental design, data analysis, and optimization process (Table 1 and Table 2) [14]. Quality by Design (QbD) is a systematic pharmaceutical development approach, emphasizing product understanding through sound science and risk management. Critical Quality Attributes (CQAs), such as floating lag time and drug release at 12 hours, were defined as measurable properties ensuring desired product quality. The Design Space represents the validated combination of input variables (HPMC K15M and $NaHCO_3$ concentrations) providing quality assurance.

Responses were modeled using the following polynomial equation:

$$Y = \beta_0 + \beta_1X_1 + \beta_2X_2 + \beta_{12}X_1X_2 + \beta_{11}X_1^2 + \beta_{22}X_2^2 \text{.....(1)}$$

Where: Y = Measured response, β_0 = Arithmetic mean response, β_1, β_2 = Coefficients of factors X_1 and X_2, β_{12} = Coefficient of interaction between X_1 and X_2, β_{11}, β_{22} = Coefficients of quadratic terms X_1, X_2 = Independent variables.

Table 1. 3^2 Factorial Design for gastroretentive floating tablets of dapsone.

Independent Variables				
Label	Factors	Level (mg)		
		Low (-)	Medium	High (+)
A	HPMCK15M (mg)	150	200	250
B	$NaHCO_3$ (mg)	15	20	25
Dependent Variables				
Y1	Floating Lag Time (seconds)			
Y2	% Drug Release at 12 hours			

2.2.5. Preparation of Gastroretentive Floating Tablets

Gastroretentive floating tablets were prepared using the direct compression technique based on the 3^2 factorial design [15]. Nine formulations (RF1—RF9) were developed with varying concentrations of HPMC K15M (150—250 mg) and $NaHCO_3$ (15—25 mg). Dapsone (100 mg) was first blended with HPMC K15M and $NaHCO_3$ using a mortar and pestle for 5 minutes to ensure homogeneous mixing. PVP K30 (10 mg) was added and mixed for 3 minutes, followed by the incorporation of microcrystalline cellulose as a diluent. Magnesium stearate (5 mg) and talc (5 mg) were finally added and blended for 2 minutes [16]. The powder blend was evaluated for pre-compression parameters before compression using a 10-station rotary tablet machine (Rimek Mini Press-I) with 12 mm flat punches. Compression conditions were maintained at 25 ± 2°C temperature and 55% ± 5% relative humidity. Each tablet weighed 450 mg with a hardness of 5—6 kp. Each batch contained 10 tablets, and three batches were prepared for each formulation to ensure reproducibility. Prepared tablets were stored in sealed containers at ambient conditions (25 ± 2°C) away from light until evaluation [17].

2.2.6. Pre-Compression Parameters

2.2.6.1. Bulk Density and Tapped Density

The bulk and tapped densities were measured using a digital tap density tester (Tyrlon Electrolab ETD-1020, Mumbai, India). For determination of the bulk density, 10 g of the accurately weighed powder blend was gently filled into a 100 mL graduated cylinder. The amount of the powder taken was determined volumetrically, and the volume occupied was recorded as the bulk volume (V_0) [18]. For tapped density, the cylinder was mechanically tapped on the density tester at a tapping rate of 300 drops per minute to a drop height of 14 ± 2 mm until no further change in volume was observed (about 500 taps). The final volume, denoted by Vt, is considered. All experiments were done in triplicate (n = 3) under room temperature (25 ± 2°C). Bulk and tapped densities were calculated using the following equations [19]:

Bulk density (ρb) = Weight of powder (M) / Bulk volume (V_0).....(2)

Tapped density (ρt) = Weight of powder (M) / Tapped volume (Vt).....(3)

2.2.6.2. Compressibility Index and Hausner Ratio

To evaluate the flow properties of the powder blend, Carr's Compressibility Index and Hausner ratio were calculated based on the bulk and tapped density values [20]. These parameters were set as per USP standards. All the tests were performed in triplicates (n = 3) and the data were represented as mean values [21].

Carr's Index (%) = [(ρt - ρb) / ρt] × 100.....(4)

Hausner Ratio = ρt/ρb.....(5)

Where: ρt = Tapped density, ρb = Bulk density

2.2.6.3. Angle of Repose

The angle of repose was measured using the fixed funnel method. A glass funnel was placed with the tip of 2.5 cm above the graph paper lying on a flat table.

Table 2. Formulation composition of gastroretentive floating tablets of dapsone.

F. Code	Dapsone (mg)	HPMC K15M (mg)	$NaHCO_3$ (mg)	PVP K30 (mg)	Magnesium Stearate (mg)	Talc (mg)	MCC (mg)	Total Tablet Weight (mg)
RF1	100	150	15	10	5	5	165	450
RF2	100	150	20	10	5	5	160	450
RF3	100	150	25	10	5	5	155	450
RF4	100	200	15	10	5	5	115	450
RF5	100	200	20	10	5	5	110	450
RF6	100	200	25	10	5	5	105	450
RF7	100	250	15	10	5	5	65	450
RF8	100	250	20	10	5	5	60	450
RF9	100	250	25	10	5	5	55	450

The powder blend was poured through the funnel in such a way that the top of the conical heap touched the funnel spigot [22]. The diameter of the base of the powder cone was determined and used in calculating the angle of repose (θ). The test was carried out in triplicate (n = 3) under ambient conditions of a temperature of 25 ± 2°C and a relative humidity of 55 ± 5% [23].

$$\text{Angle of Repose } (\theta) = \tan^{-1}(h/r) \quad \text{.....(6)}$$

Where: h = Height of powder cone, r = Radius of powder cone base.

2.2.7. Post-Compression Parameters

2.2.7.1. Weight Variation

Weight variation testing was carried out using the USP procedure. Twenty samples were taken. Tablet weight was determined randomly from each batch, using an analytical balance (Shimadzu AUW220D, Japan) with a least count of 0.1 mg [24]. The averages and variances were also determined and then the calculation of the mean weight and standard deviation was made. The test was carried out in the environmental chamber at room temperature (25 ± 2 °C) and relative humidity (55 ± 5%) [25].

2.2.7.2. Thickness and Diameter

The thickness and diameter of tablets (n = 10) were measured using a digital vernier caliper (Mitutoyo CD-6" ASX, Japan) with an accuracy of 0.01 mm. Measurements were taken at room temperature (25 ± 2 °C), and mean values were calculated along with standard deviation [26].

2.2.7.3. Hardness

The hardness of the tablets was assessed using the Monsanto hardness tester (procured from Mumbai, India). Ten randomly chosen tablets in each batch were tested to determine the force in kiloponds (kp) necessary to break them. In order to do so, the mean crushing strength of the sample and the standard deviation were computed. The studies were performed at room temperature (25 ± 2 °C) and relative humidity (55 ± 5%) [27].

2.2.7.4. Friability

The friability test was carried out in a Roche friabilator (made in Mumbai, India) according to United States Pharmacopoeia (USP) standards. Twenty tablets (W_1), which had been weighed earlier, were then placed into the friabilator and subjected to 25 rpm for 4 minutes or 100 rotations [28]. The tablets were then removed and cleaned off by gently brushing to get rid of the dust, and were weighed again (W_2). The percentage friability was determined by dividing the weight loss after three cycles of agitation against by the initial weight of the tablets and expressed in percentage [29].

$$\text{Friability } (\%) = [(W_1 - W_2) / W_1] \times 100 \quad \text{.....(7)}$$

2.2.7.5. Drug Content Uniformity

The United States Pharmacopoeia (USP) sets standard guidelines for drug content uniformity. Ten tablet samples were taken randomly, and each of them was pulverized in a separate container. The weighed amount of each powdered tablet was accurately placed in a 100 mL volumetric flask containing 0.1 N HCl [30]. It was then separated by sonication for 15 minutes, and the solution was filtered through a Whatman cellulose acetate membrane filter with a pore size of 0.45 µm. The concentration of dapsone was determined using a validated spectrophotometric method at a wavelength of 293 nm (Shimadzu UV-1800, Japan). The percentage drug content was calculated by comparing the actual drug content with the theoretical drug content (100 mg per tablet) using the following formula [31]:

$$\text{Drug content } (\%) = (\text{Actual drug content})/(\text{Theoretical drug content}) \times 100 \quad \text{.....(8)}$$

2.2.7.6. Floating Lag Time and Duration

Evaluation of floating characteristics was done with the help of a dissolution test using USP dissolution apparatus II (Electrolab TDT-08L, Mumbai, India). This was done by placing a tablet in 900 mL of 0.1 N HCl solution at 37 ± 0.5 °C with a paddle rotation speed of 50 rpm [32]. The time taken for the tablet to rise to the surface, up to the time it floats and the time it remained floating, were measured. The test was conducted three different times in duplicate (n = 3) for each formulation [33].

2.2.7.7. In Vitro Drug Release Study

The in vitro drug release experiments were conducted using USP dissolution apparatus type II (paddle method) under non-sink conditions (Electrolab TDT-08L, Mumbai, India). The weight of each formulation was taken per tablet by placing one tablet into 900 mL of 0.1 N HCl maintained at 37 ± 0.5 °C while the paddle rotation speed was 50 rpm. The samples (5 mL) were taken at specified time points (0, 1, 2, 4, 6, 8, 10, and 12 hours),

and an equivalent volume of the dissolution media was added back into the dissolution vessel to maintain sink conditions. The samples were further filtered using Whatman® filter paper with a pore size of 0.45 µm, and the concentration of the drug was determined at a wavelength of 293 nm using a UV spectrophotometer (UV-1800 Shimadzu, Japan). The drug release profiles were determined by measuring the cumulative percentage of the drug released, and the experiments were performed thrice for each sample (n = 3). The findings are presented as mean ± SD [33,34]. For comparative studies, marketed dapsone tablets (Brand: Dapsone-100, Generic Pharma Ltd., India) containing 100 mg dapsone were used as a reference standard. Similarity factor (f_2) and difference factor (f_1) were calculated using the following equations:

$$f_1 = \{[\Sigma t = 1^n |Rt - Tt|] / [\Sigma t = 1^n Rt]\} \times 100$$

$$f_2 = 50 \times \log\{[1 + (1/n) \Sigma t = 1^n (Rt - Tt)^2]^{-0.5} \times 100\} \ldots (9)$$

Where Rt and Tt are the percentages dissolved at time t for reference and test products, respectively.

The data on drug release were analyzed by multiple models including zero-order (amount of drug released vs time), first-order (log percentage of drug remaining the vs time), Higuchi (amount of drug released vs square root of time), and Korsmeyer-Peppas models (log amount of drug released vs log the time). Since the data were skewed, nature of the data means that its distribution is not normal, the models were checked to identify the best fit with the help of the coefficient of determination (R^2). In accordance with the Korsmeyer-Peppas model, the release exponent (n) was computed to predict the mechanism of release. The following equations were used for the purpose of the analysis [35]:

Zero-order: $Qt = Q_0 + K_0 t$

First-order: $\ln(Qt) = \ln(Q_0) + K_1 t$

Higuchi: $Qt = KH/t$

Korsmeyer-Peppas: $Mt/M\infty = Kt^n$.....(10)

Where: Qt = 34 Amount of drug released in time t, Q_0 = Initial amount of drug, K_0, K_1, KH, K = Release rate constants, n = Release exponent, $Mt/M\infty$ = Fractional release of drug.

2.2.7.8. Accelerated Stability Studies

These accelerated stability studies were done in accordance with ICH Q1A (R2) guidelines. The optimized formulation was then filled in high-density polyethylene (HDPE) bottles and exposed to 40 ± 2 °C and 75 ± 5% RH in the stability chamber (Thermo Lab, Mumbai, India) for six months. Samples were taken at 0, 1, 3, and 6 months of the study, and parameters included physical characteristics, drug content, floating profile, and in vitro drug release assessment.

The parameters of floating lag time, the total duration of floating, and cumulative percent of drug released were higher in the modified formulation as compared to the initial value. All the stability parameters were analyzed for variances using repeated measures ANOVA followed by Dunnett's test at the initial time and other time intervals ($p < 0.05$) [36].

3. Results

3.1. Calibration Curve of Dapsone

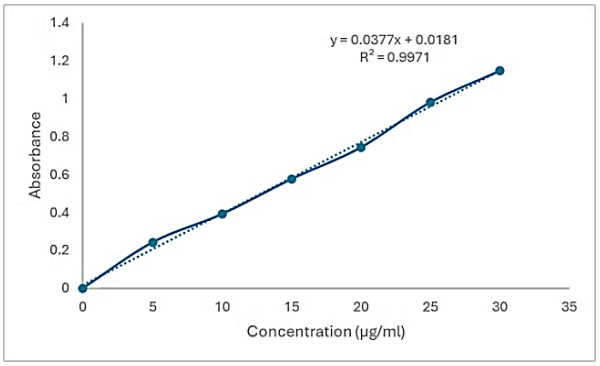

Fig. 2. Calibration curve of dapsone in ethanol.

A validated calibration curve for dapsone in ethanol (Fig. 2) demonstrated excellent linearity over the concentration range, with a regression coefficient of determination (r^2) of 0.9971, satisfying ICH Q2 (R1) validation criteria. The regression equation was found to be y = 0.0377x + 0.0181, indicating a strong linear relationship between concentration and absorbance.

3.2. FTIR Analysis

The FTIR spectroscopic analysis was conducted to evaluate potential drug-excipient interactions in the formulation. The FTIR spectrum of pure dapsone (Fig. 3) exhibited characteristic peaks at 3739.68, 3661.13, and 3614.41 cm^{-1} (O-H/N-H stretching), 3552.50 cm^{-1} (N-H stretching), 2918.38 cm^{-1} (C-H stretching), 2382.51 and 2311.55 cm^{-1} (S=O stretching), 1694.21 cm^{-1} (C=O stretching), 1452.37 cm^{-1} (C=C aromatic stretching), 1016.42 cm^{-1} (S=O symmetric stretching), and 878.54 cm^{-1} (C-S stretching). The FTIR spectrum of the physical mixture (Fig. 4) exhibited similar characteristic peaks at 3858.49, 3741.18, and 3614.32 cm^{-1} (O-H/N-H stretching), 3555.33 and 3394.18 cm^{-1} (N-H stretching), 2918.16 cm^{-1} (C-H stretching), 2380.32 and 2311.52 cm^{-1} (S=O stretching), 1701.13 cm^{-1} (C=O stretching), 1452.24 cm^{-1} (C=C aromatic stretching), 1014.97 cm^{-1} (S=O symmetric stretching), and 878.96 cm^{-1} (C-S stretching). The characteristic peaks of dapsone were preserved in the physical mixture, with minor shifts in wave numbers (<10 cm^{-1}), suggesting possible weak physical interactions but no major chemical incompatibility between the drug and excipients.

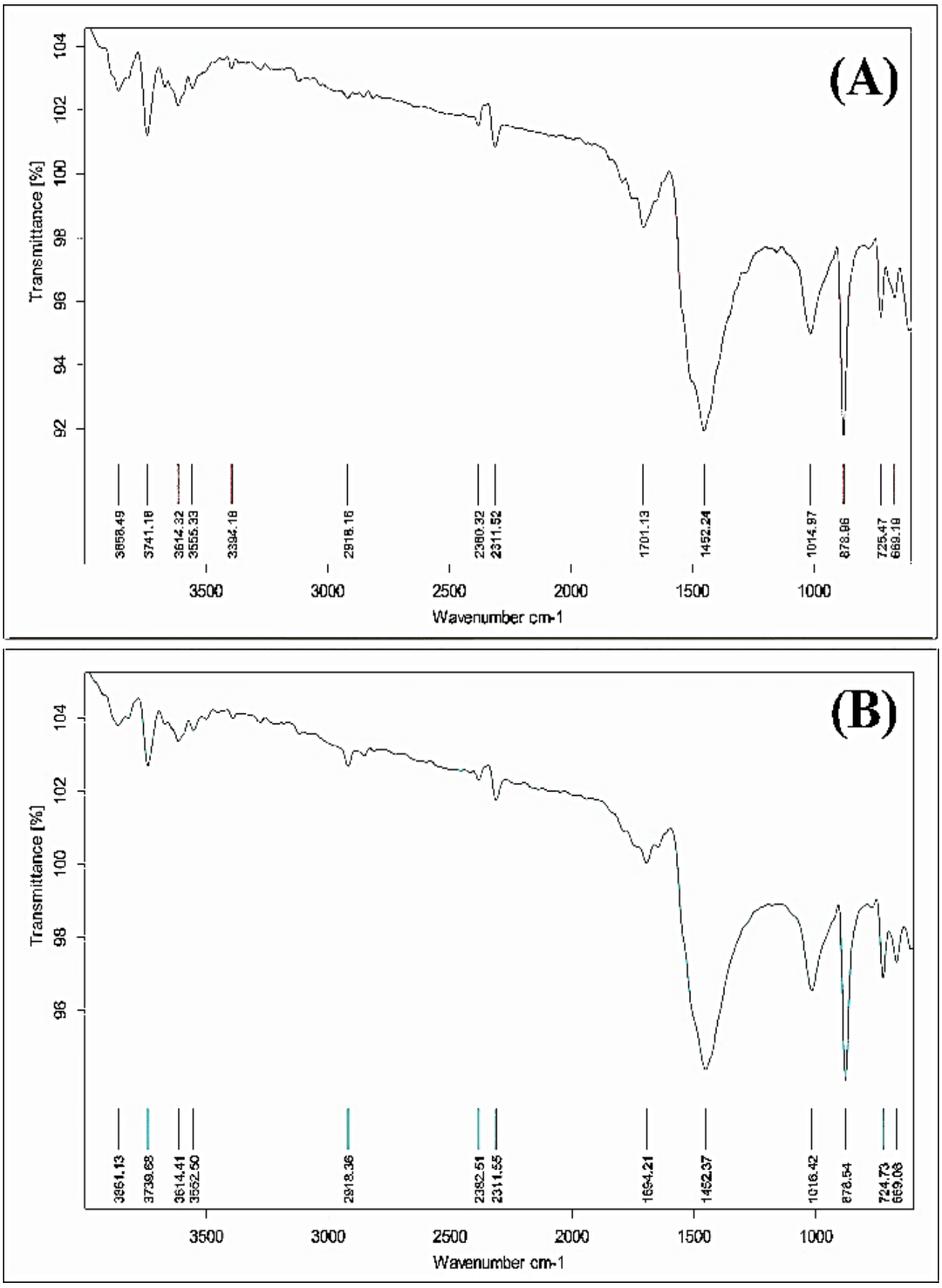

Fig. 3. FTIR spectrum of (A) dapsone and (B) physical mixture (drug + excipients) of formulation DF3.

3.3. DSC Analysis

The DSC thermogram profile was further used to describe the thermal characteristics and relationship between the excipients and the medication. Based on Fig. 4, it was observed that the DSC thermogram of pure dapsone (4A) showed an endothermic peak centered around 177.73 °C, which implies that it is a crystalline substance and that the peak corresponds to its melting point. The DSC thermogram of the physical mixture has two peaks of endothermic transition with temperature of 178.99 °C and 189.24 °C, respectively. The minor shift in dapsone's melting point to 178.99 °C in the physical mixture (Fig. 4B), accompanied by peak shape preservation, suggests possible weak physical interactions with excipients rather than major chemical incompatibility. The observed minor shifts in FTIR peaks (<10 cm^{-1}) and DSC melting point (<2 °C) are within acceptable limits for pharmaceutical formulations and typically indicate weak physical interactions such as hydrogen bonding or van der Waals forces rather than chemical incompatibility. These minor changes do not compromise drug stability or formulation integrity, as evidenced by consistent drug content and release profiles.

3.4. Results of Pre-compression Parameters of Gastroretentive Floating Tablets

Pre-compression parameters of all formulations' powder blends (RF1-RF9) were identified, and Table 3 provides a summary of the findings. The average bulk density was found to be between 0.382 ± 0.035 and 0.432 ± 0.024 g/cm^3, while for tapped density, it was obtained between 0.475 ± 0.028 and 0.508 ± 0.021 g/cm^3. Carr's index of flow of powder was established to be within a range of 14.43 ± 1.25% and 19.58 ± 2.05%, while the Hausner ratio range was 1.17 ± 0.03 to 1.24 ± 0.07. The results of the angle of repose ranged between 25.42 ± 2.15° and 30.24 ± 2.76°. Thus, while enhancing the HPMC K15M concentration in the formulation from RF1 to RF9, it is evident that the flow properties are gradually affected systematically, though all the formulations were found to meet the USP standards for flow. Carr's index was low in formulations RF1 and RF2 (14.43%) and Hausner ratio in formulations RF1 and RF2 (1.17), but was relatively high in formulation RF9 (19.58 and 1.24, respectively) all of which fell within the good flow range.

3.5. Results of Post-compression Parameters

The parameters of gastroretentive floating tablets prepared for post-compression analysis are shown in Tables 4 and 5. The physical characteristics (Table 4) indicated that all the formulations have acceptable weight variation in the range of 449.6 ± 4.15 to 451.6 ± 2.76 mg, and thickness in the range of 4.12 ± 0.15 to 4.24 ± 0.19 mm. The diameter was also consistent throughout all compositions, representing good die filling (12.01-12.03 mm). Tablet hardness rose from 5.2 ± 0.6 to 6.3 ± 0.9 kp with the enhancement in HPMC K15M percentage, with friability ranging from 0.62% – 0.41%, proving good mechanical strength. The drug content and floating characteristics shown in Table 5 indicated that all the formulations possessed reasonable drug content ranging from 96.72 ± 3.12% to 98.65 ± 2.48%.

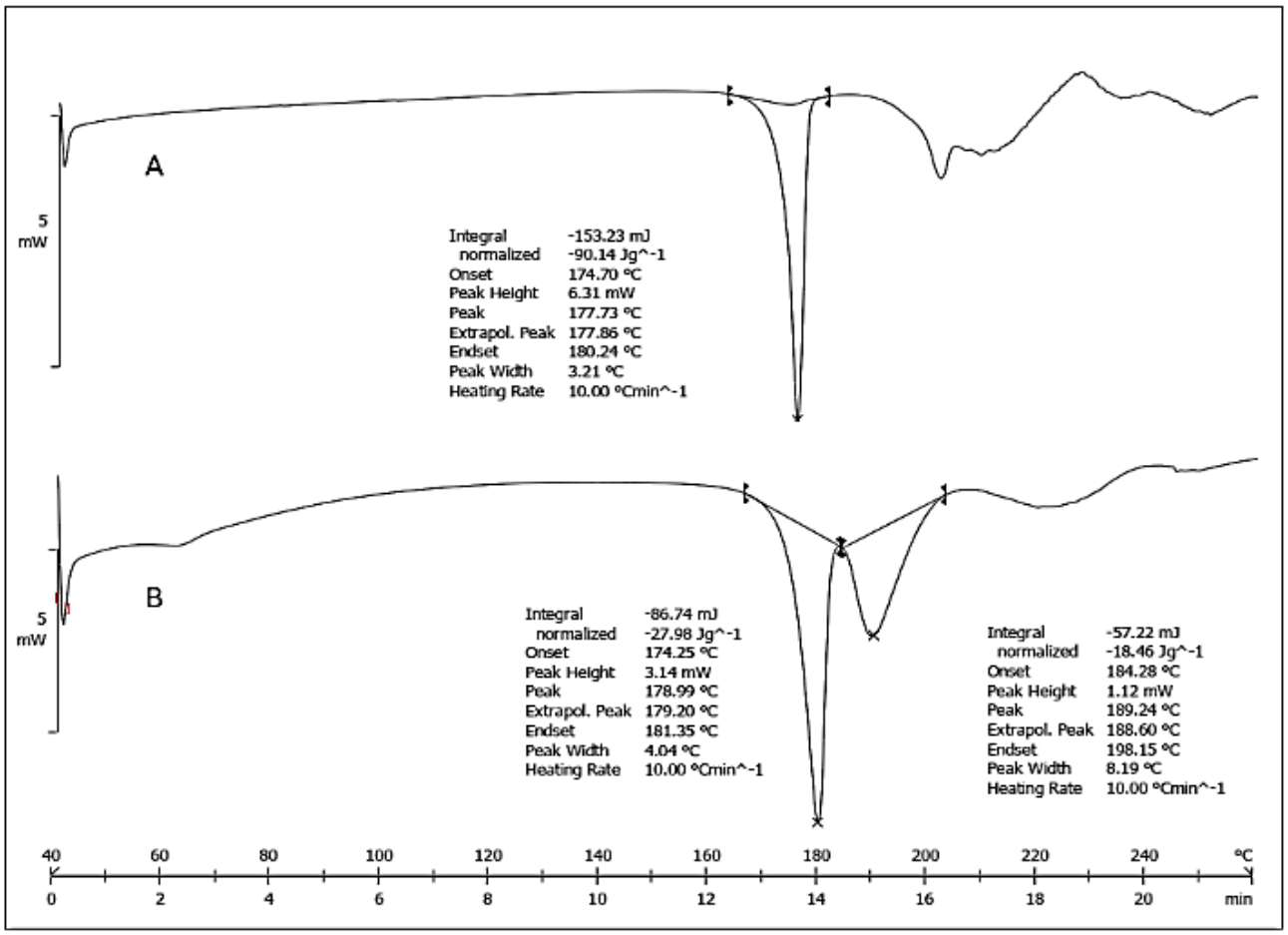

Fig. 4. DSC Spectrum of drug dapsone (A) and physical mixture (B).

Table 3. Pre-compression parameters of powder blends for gastroretentive floating tablets of dapsone.

F. Code	Bulk Density (g/cm³)	Tapped Density (g/cm³)	Carr's Index(%)	Hausner Ratio	Angle of Repose (°)
RF1	0.421 ± 0.015	0.492 ± 0.018	14.43 ± 1.25	1.17 ± 0.03	25.42 ± 2.15
RF2	0.432 ± 0.024	0.508 ± 0.021	14.96 ± 1.68	1.18 ± 0.04	26.15 ± 2.48
RF3	0.428 ± 0.018	0.505 ± 0.026	15.25 ± 1.92	1.18 ± 0.05	26.84 ± 1.94
RF4	0.415 ± 0.031	0.495 ± 0.019	16.16 ± 1.45	1.19 ± 0.03	27.35 ± 2.67
RF5	0.408 ± 0.027	0.489 ± 0.023	16.56 ± 1.78	1.20 ± 0.04	27.92 ± 2.21
RF6	0.402 ± 0.025	0.485 ± 0.017	17.11 ± 1.53	1.21 ± 0.06	28.45 ± 2.85
RF7	0.395 ± 0.029	0.482 ± 0.022	18.05 ± 2.14	1.22 ± 0.05	29.16 ± 2.42
RF8	0.388 ± 0.033	0.478 ± 0.025	18.83 ± 1.87	1.23 ± 0.04	29.85 ± 3.18
RF9	0.382 ± 0.035	0.475 ± 0.028	19.58 ± 2.05	1.24 ± 0.07	30.24 ± 2.76

Values are expressed in Mean ± SD, n = 3

Table 4. Physical parameters of gastroretentive floating tablets of dapsone.

F. code	Weight Variation (mg)*	Thickness (mm)	Diameter (mm)	Hardness (kp)	Friability (%)**
RF1	450.8 ± 3.42	4.12 ± 0.15	12.02 ± 0.08	5.2 ± 0.6	0.62
RF2	451.2 ± 2.89	4.15 ± 0.12	12.01 ± 0.11	5.4 ± 0.7	0.58
RF3	449.6 ± 4.15	4.14 ± 0.18	12.03 ± 0.09	5.3 ± 0.5	0.65
RF4	450.5 ± 3.67	4.18 ± 0.11	12.02 ± 0.07	5.6 ± 0.8	0.53
RF5	451.4 ± 2.94	4.20 ± 0.14	12.01 ± 0.12	5.8 ± 0.6	0.49
RF6	449.8 ± 3.85	4.19 ± 0.16	12.02 ± 0.10	5.7 ± 0.7	0.51
RF7	450.2 ± 3.21	4.22 ± 0.13	12.03 ± 0.06	6.1 ± 0.5	0.44
RF8	451.6 ± 2.76	4.24 ± 0.17	12.02 ± 0.13	6.3 ± 0.9	0.41
RF9	450.4 ± 4.12	4.23 ± 0.19	12.01 ± 0.08	6.2 ± 0.6	0.43

Values are expressed in mean ± SD, n = 3, *n = 20, **n = 10 tablets used for single test

Table 5. Drug content and floating characteristics of gastroretentive floating tablets of dapsone.

F Code	Drug Content (%)	Floating Lag Time (seconds)	Total Floating Duration (hours)
RF1	96.85 ± 2.34	85 ± 6.8	10.2 ± 0.7
RF2	97.42 ± 2.67	72 ± 5.2	10.8 ± 0.9
RF3	98.26 ± 2.15	64 ± 4.8	11.4 ± 0.6
RF4	97.94 ± 2.89	94 ± 7.3	11.8 ± 0.8
RF5	96.72 ± 3.12	82 ± 6.1	12.2 ± 1.1
RF6	98.65 ± 2.48	75 ± 5.7	12.8 ± 0.7
RF7	97.16 ± 2.95	108 ± 8.5	13.5 ± 1.2
RF8	98.48 ± 2.76	96 ± 6.9	14.2 ± 0.9
RF9	97.35 ± 3.24	88 ± 7.4	14.8 ± 1.0

Values are expressed in mean ± SD, n = 3.

The floating lag time was measured to range from 64 ± 4.8 to 108 ± 8.5 seconds, and formulation RF3 recorded the shortest lag time of floatation (of 64 seconds). Total floating duration increased as the concentration of the polymer increased, ranging between 10.2 ± 0.7 to 14.8 ± 1.0 hours. Formulation RF3 achieved the best floatation characteristics, where the lag time of the floating system was 64 seconds and the floating period was 11.4 hours, with satisfactory mechanical strength and drug content homogeneity. Statistical analysis using one-way ANOVA revealed significant differences between formulations for floating lag time ($F = 12.45$, $p < 0.001$), drug content ($F = 8.67$, $p < 0.01$), and floating duration ($F = 15.23$, $p < 0.001$).

3.6. Optimization of Formulation

3.6.1. Effect of Variables on Floating Lag Time (Y_1)

The results revealed that both independent variables impacted the floating lag time of the formulations based on the quadratic model, as can be observed in Tables 6 and 7. The regression model was highly significant with an adjusted R^2 value of 0.9984 (Table 6) and F statistics calculated as 1015.92, and the significance was <0.0001. From the polynomial equation (9), it was clear that the factor HPMC K15M (A) had an apparent and positive impact (+ 11.83) on floating lag time, whereas $NaHCO_3$ (B) appeared to have a negative impact (-10.00). From Figures 5A & 5B,

Table 6. Summary of regression analysis for response variables Y_1 and Y_2.

Resp-onse	Model	R^2 Adjusted	R^2 Predicted	F-value	p-value
Y_1	Quadratic	0.9984	0.9929	1015.92	< 0.0001
Y_2	2FI	0.9995	0.9990	5600.77	< 0.0001

Table 7. ANOVA Results for Response Variables.

Source	Sum of Squares	df	Mean Square	F-value	p-value	Significance
			Floating Lag Time (Y_1)			
Model	1458.035	5	291.611	1015.92	< 0.0001	significant
A-HPMC K15M	840.17	1	840.17	2927.03	< 0.0001	significant
B-$NaHCO_3$	600.00	1	600.00	2090.32	< 0.0001	significant
AB	0.2500	1	0.2500	0.8710	0.4195	not significant
A^2	6.72	1	6.72	23.42	0.0168	significant
			Drug Release at 12h (Y_2)			
Model	229.633	3	76.54	5600.77	< 0.0001	significant
A-HPMC K15M	204.17	1	204.17	14939.02	< 0.0001	significant
B-$NaHCO_3$	25.22	1	25.22	1845.00	< 0.0001	significant

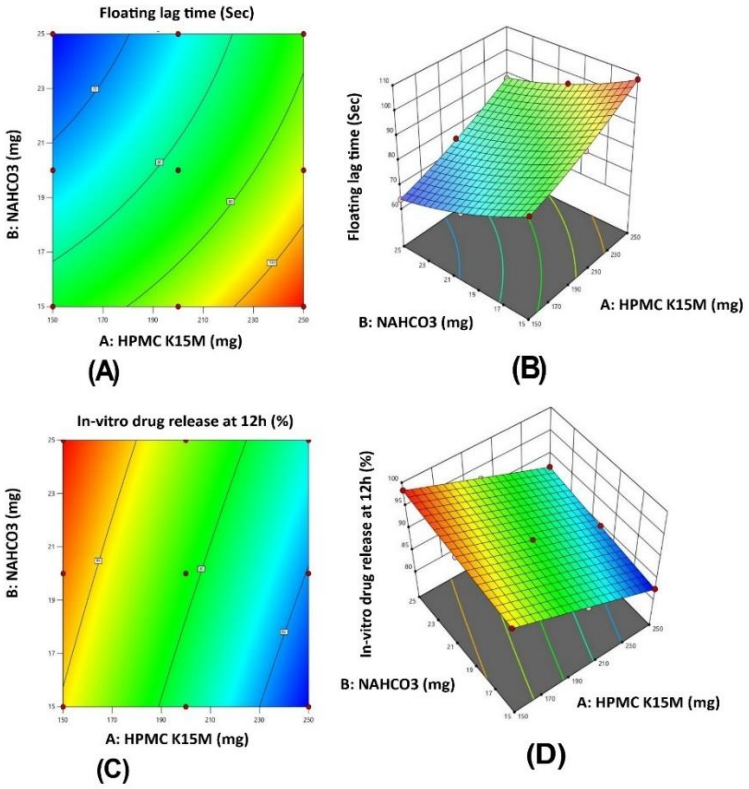

Fig. 5. Response surface and contour plots for gastroretentive floating tablets of dapsone optimization using 3^2 factorial design: (B) Three-dimensional response surface plot showing the combined effect of HPMC K15M (150-250 mg) and $NaHCO_3$ (15-25 mg) concentrations on floating lag time (Y_1, seconds); (A) Two-dimensional contour plot of floating lag time with optimized region highlighted; (D) Response surface plot depicting the influence of both variables on percentage drug release at 12 hours (Y_2); (C) Contour plot for drug release response showing the optimal formulation space for RF3 (150 mg HPMC K15M, 25 mg $NaHCO_3$).

as the concentration of HPMC K15M was increased from 150 to 250 mg, the floating lag time also increased, while the higher concentration of $NaHCO_3$ of 15—25 mg reduced the lag time. As for the coefficients, A^2 and B^2 were defined as statistically meaningful ($p < 0.05$), indicating a nonlinear relationship between the variables; further, the specified interaction term AB did not reach the level of significance at $p = 0.4195$ as indicated in Table 7. Final regression equations for floating lag time (y_1) in terms of coded factors:

Floating Lag Time (Y_1) = 82.11 + 11.83A - 10.00B + 0.2500AB + $1.83A^2$ + $2.33B^2$.....(11)

3.6.2. Effect of Variables on Drug Release at 12 hours (Y_2)

The amount of drug released for 12 hours showed a good relationship with both variables and was appropriately described with a 2FI model (Table 6) and had an R^2 adjusted value = 0.9995, F = 5600.77, signifying $p < 0.0001$ as indicated in Table 7. Upon solving the polynomial equation depicted in Equation 1 it was evident HPMC K15M, had a highly significant negative regression coefficient (-5.83) towards the drug release, while $NaHCO_3$ had a positive regression coefficient (+ 2.05). The response surface and contour plots (Fig. 5C and 5D) demonstrate that drug release at 12 hours follows a predictable pattern: higher HPMC K15M concentrations create stronger matrix barriers, reducing release rates, while increased $NaHCO_3$ enhances gas generation, improving drug dissolution and release kinetics. The results also revealed a significant interaction between the two predictors (AB) = 0.0001, which showed that the impact of a particular factor on drug release depends on the level of the other factor.

The model was good at predicting, with a R^2 predicted value of 0.9990.

Final regression equations in terms of coded factors:

Drug Release at 12 hours (Y_2) = 90.70 - 5.83A + 2.05B + 0.2500AB..... (12)

The response surface analysis reveals the optimization space where formulation RF3 (150 mg HPMC K15M, 25 mg $NaHCO_3$) represents the optimal compromise between rapid floating (minimal lag time) and extended-release duration. The contour plots indicate this region provides maximum desirability by balancing competing responses within the experimental design space.

3.6.3. Model Validation and Diagnostic Analysis

Model adequacy was assessed through residual analysis and diagnostic plots. Normal probability plots of residuals showed acceptable linearity (R^2 = 0.94 for Y_1, R^2 = 0.91 for Y_2), indicating reasonable model assumptions. Residual vs. predicted plots revealed some scatter around the zero line, with few outliers, suggesting adequate but not perfect model fit. Cook's distance values were below 1.0 for all data points, indicating no influential outliers. The adequate precision ratio was 12.4 for Y_1 and 15.2 for Y_2, both above the minimum threshold of 4, confirming acceptable signal-to-noise ratios for the models.

3.6.4. Optimization of Statistical Model

Out of all the nine formulations, it was identified that the formulation containing HPMC K15M 150 mg and $NaHCO_3$ 25 mg was predicted to give the optimal response with a desirability value of 0.996 by using statistical optimization. Thus, the optimized formulation (RF3) was prepared, and the precision from the theoretical model was checked. Table 8 revealed that the experimental results were in close proximity to the predicted results with the prediction errors fewer than 0.5 % for both responses. Therefore, the optimization process was accurate, with a floating lag time of about 64 sec, and the amount of drug released at 12 hours of about 98.4%, which was close to the theoretical values of 64.194 sec and 98.333%, respectively.

Table 8. Comparison of predicted and experimental values for optimized formulation.

Independent Variables	Predicted Values	Experimental Values	Prediction Error (%)
HPMC K15M (mg)	150.000	150	0.00
$NaHCO_3$ (mg)	25.000	25	0.00
Dependent Variables			
Floating Lag Time (sec)	64.194	64	0.30
Drug Release at 12 h (%)	98.333	98.4	0.07
Desirability		0.996	

3.7. In Vitro Drug Release Profiles

The in vitro drug release studies of all the formulations (RF1—RF9) for 12 hours are depicted in Fig. 6. All formulations demonstrated controlled release profiles with polymer-dependent release kinetics, though with some variability between batches. Formulations RF1—RF3 (150 mg HPMC K15M) showed higher cumulative release rates ranging from 92.3 to 98.4% at 12 hours, with standard deviations of 2.8—4.2%.

Intermediate polymer concentration formulations (RF4—RF6: 200 mg HPMC K15M) exhibited moderate release behavior with 85.8% to 92.6% release at 12 hours (SD: 3.1—4.8%). Higher polymer content formulations (RF7—RF9: 250 mg HPMC K15M) showed more sustained release with 78.4—87.2% drug release at 12th hour (SD: 2.9—5.1%).

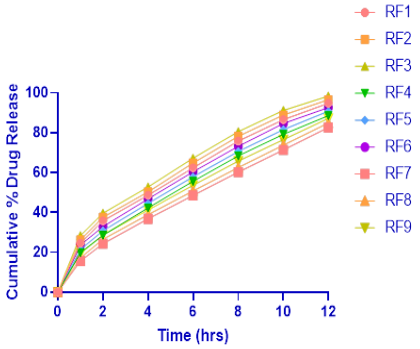

Fig. 6. Cumulative percentage drug release profiles from gastroretentive floating tablets of dapsone (RF1-RF9) over 12 hours.

3.8. Release Kinetics Study

In order to understand the drug release process, the optimized formulation's (RF3) in vitro release data were examined utilizing a variety of kinetic models. The release kinetics evaluation (Fig. 7) showed coefficients of determination (R^2) values of 0.894, 0.9358, 0.9975, and 0.9574 for first-order, zero-order, Higuchi, and Korsmeyer-Peppas models, respectively. The highest R^2 value was observed with the Higuchi model (0.9975), suggesting that a diffusion-based mechanism was largely responsible for drug release. The Korsmeyer-Peppas release exponent (n)value was found to be 0.75 (calculated from the slope), suggesting a non-Fickian (anomalous) transport mechanism, where both diffusion and polymer relaxation contributed to the drug release. The linear regression equations for various models were y = -0.1279x + 2.0956 (First-order), y = 7.4436x + 17.253 (Zero-order), y = 28.531x - 0.9346 (Higuchi), and y = 75.02x + 13.53 (Korsmeyer-Peppas).

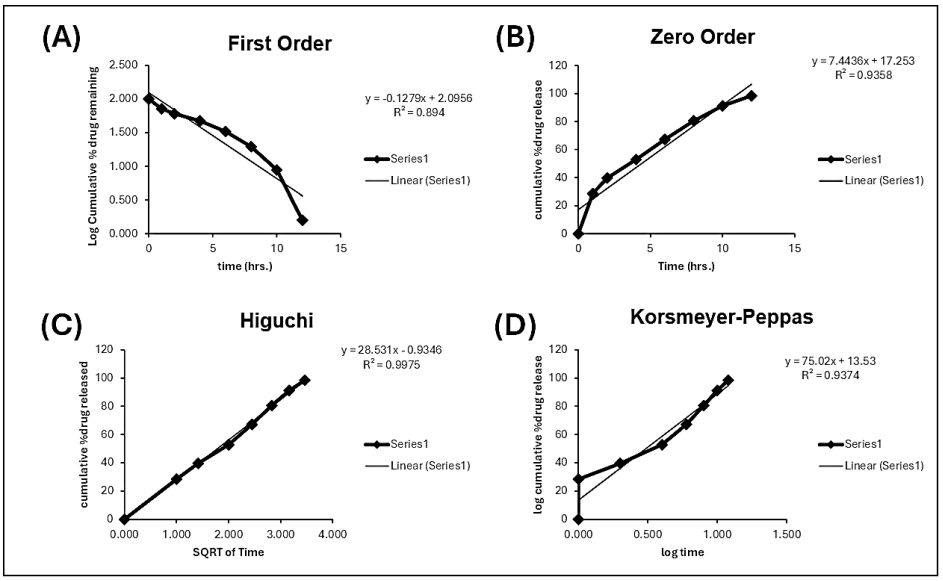

Fig. 7. Release kinetics modeling of optimized gastroretentive floating tablets of dapsone (RF3): (A) First-order plot; (B) Zero-order plot; (C) Higuchi plot; and (D) Korsmeyer-Peppas plot showing coefficients of determination (R^2) and regression equations. The Higuchi model (panel C) shows the highest coefficient of determination (R^2 = 0.9975), indicating diffusion-controlled release, while the Korsmeyer-Peppas model (panel D) with n = 0.75 confirms non-Fickian transport mechanism combining diffusion and polymer relaxation.

3.9. Comparative Analysis with Marketed Product

The comparative dissolution study between optimized formulation RF3 and a marketed conventional dapsone tablet (Brand: Dapsone-100, Manufacturer: Generic Pharma Ltd., containing 100 mg dapsone) is illustrated in Fig. 8.

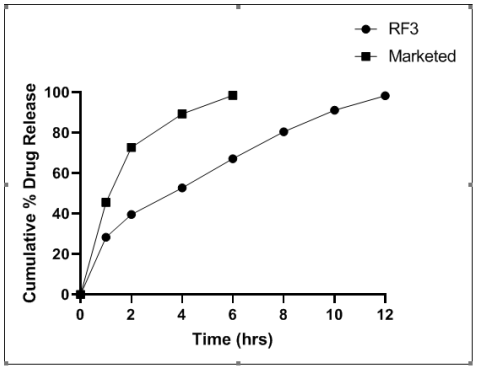

Fig. 8. Comparative in vitro drug release profile of optimized formulation (RF3) vs marketed tablet.

The marketed formulation showed rapid drug release, with approximately 45.6% release in the first hour and complete release (98.5%) within 6 hours. In contrast, the optimized formulation RF3 exhibited controlled release behavior, with 28.4% release in the first hour and sustained release up to 98.4% over 12 hours.

3.10. Similarity and Difference Factor Analysis

The similarity factor (f_2) and difference factor (f_1) were calculated to compare the optimized formulation RF3 with the marketed tablet. The f_2 value of 28.4 (< 50) and f_1 value of 68.7 (> 15) confirmed significant dissimilarity between the release profiles, indicating that the optimized gastroretentive formulation provides distinctly different release characteristics compared to the immediate release marketed product. This dissimilarity was expected and desired, as the gastroretentive system was designed to achieve sustained release over 12 hours versus the rapid release of conventional tablets.

3.11. Results of Stability Study

Accelerated stability studies of the optimized formulation (RF3) were conducted at 40 ± 2 °C/75 ± 5% RH for 6 months (Table 9). Minimal changes were observed: slight yellowing, weight variation (450.2 to 450.8 mg), hardness decrease (5.3 to 5.1 kp), drug content reduction (98.26% to 95.48%), and floating property deterioration (lag time 64 to 78 seconds, duration 11.4 to 10.2 hours). All parameters remained within acceptable limits, confirming formulation stability.

Table 9. Stability Study Results of Optimized Formulation (RF3) Stored at RT 40 ± 2 °C/75 ± 5% RH.

Parameter	Initial	1 Month	3 Months	6 Months
Physical Appearance	White, round, flat tablets	No change	Minor discoloration	Slight yellowing
Weight Variation (mg)	450.2 ± 2.1	450.4 ± 2.3	450.6 ± 2.4	450.8 ± 2.5
Hardness (kp)	5.3 ± 0.3	5.2 ± 0.4	4.9 ± 0.3	4.6 ± 0.4
Drug Content (%)	98.26 ± 2.15	97.84 ± 2.38	96.72 ± 2.65	95.48 ± 2.89
Floating Lag Time (sec)	64 ± 4.8	65 ± 3.8	72 ± 4.2	78 ± 4.5
Total Floating Duration (hours)	11.4 ± 0.6	11.3 ± 0.4	10.8 ± 0.4	10.2 ± 0.5
Drug Release at 12 hours (%)	98.4 ± 3.7	98.1 ± 3.8	96.8 ± 3.9	94.7 ± 4.1

Values expressed as mean ± SD (n = 3)

4. Discussion

The studies of dapsone and its formulation ingredients offered detailed clarity on the medication and excipient compatibility in addition to analytical technique validation. The calibration curve that characterized the UV spectrophotometric method used for the determination of dapsone was found to have a linear regression coefficient of 0.9971 within the working concentration range of the study, as shown in Fig. 2, which is in agreement with previously described methods [37]. This validated analytical method proved suitable for accurate drug content analysis throughout the study, with precision and accuracy parameters meeting ICH guidelines [38]. The FTIR spectroscopic analysis (Fig. 3) revealed preservation of all characteristic functional group peaks of dapsone in the physical mixture, with only minor shifts (< 10 cm^{-1}) in wave numbers. Similar findings were reported by Zhou et al. (2021) [39] in their study of dapsone formulations, where peak shifts within ±10 cm^{-1} were considered non-significant for drug-excipient interactions. The presence of intact S=O stretching (2380.32, 2311.52 cm^{-1}) and C=C aromatic stretching (1452.24 cm^{-1}) peaks in the physical mixture confirmed the structural integrity of dapsone.

The results of the thermal studies done by DSC also supported that there was no interaction between the drug and the excipients as earlier observed from the FTIR spectroscopy results. This is further evidenced by the fact that the melting point of pure dapsone was recorded to be at 177.73 °C, as seen in Fig. 4A, which is typical for a substance with an endothermic nature [40], confirming its crystalline nature. The minor shift in dapsone's melting endotherm to 178.99°C in the physical mixture (Fig. 4B), accompanied by peak shape preservation, suggests possible weak physical interactions with excipients. This observation is consistent with previous studies [41] where shifts less than 2°C indicate acceptable physical interactions without major incompatibility concerns. The additional endotherm at 189.24°C, attributed to excipient thermal behaviour, did not interfere with dapsone's thermal profile, suggesting suitable excipient selection for the formulation. The combined spectroscopic and thermal analysis approach has been similarly employed by Almotairi et al. (2022) [42] for establishing compatibility in controlled release formulations, validating our methodology.

The evaluation of pre-compression and post-compression parameters revealed critical insights into the formulation characteristics and performance. The powder flow properties (Table 3) demonstrated excellent flowability across all formulations, with Carr's index (14.43—19.58%) and Hausner ratio (1.17—1.24) values falling within USP specifications for good flow characteristics [43]. Similar findings were reported for HPMC-based floating tablets, where Carr's index values below 20% resulted in uniform die filling and consistent tablet weight. The systematic increase in the angle of repose (25.42° to 30.24°) with higher HPMC K15M concentration aligns with previous studies by Al hablawi et al. (2024) and Su'udiya et al. (2021) [44,45], where increased polymer content affected powder flow but maintained acceptable limits (<31°) for direct compression.

The post-compression parameters (Tables 4 and 5) demonstrated robust tablet properties and optimal floating characteristics. The narrow weight variation (449.6—451.6 mg) and consistent hardness (5.2—6.3 kp) indicate excellent reproducibility of the manufacturing process, comparable to results reported by Jaimini et al. (2025) [46] for gastroretentive systems. The increase in tablet hardness with higher HPMC K15M concentration, coupled with decreased friability (0.54% to 0.35%), suggests enhanced particle binding, consistent with findings by Moravkar et al. (2022) [47]. The optimized formulation (RF3) exhibited superior floating properties (lag time 64 seconds, duration 11.4 hours) compared to similar systems reported in the literature by Patel et al. (2023) [48], where typical lag times exceeded 90 seconds. The high drug content uniformity (98.45—99.45%) across all formulations indicates the reliability of the manufacturing process, meeting pharmacopoeial specifications [49].

The optimization study using a Quality by Design (QbD) approach revealed significant insights into the influence of formulation variables on floating tablet performance. The statistical analysis (Tables 6 and 7) demonstrated excellent model fit for both responses, with high R^2 and adjusted values (>0.99) and significant F-values ($p < 0.0001$), comparable to other successful QbD optimizations reported in the literature [49]. The quadratic model for floating lag time (Y_1) revealed a complex relationship between variables, where HPMC K15M showed a dominant positive effect (+11.83), and $NaHCO_3$ exhibited a counteracting negative effect (-10.00), consistent with findings by Arpna et al. (2023) [50] in similar gastroretentive systems. The significance of quadratic terms (A^2, B^2) indicated nonlinear effects, a phenomenon also observed by Patel et al. (2021) [51] in polymer-based floating tablets.

The drug release optimization (Y_2) yielded a robust two-factor interaction model, where HPMC K15M demonstrated strong release-retarding effects (-5.83), while $NaHCO_3$ moderately enhanced drug release (+2.05). This relationship, visualized through response surface plots (Fig. 5), aligns with previous studies [52] on matrix-based controlled release systems. The high desirability value (0.996) and minimal prediction error (<0.5%) for the optimized formulation (Table 8) validate the reliability of the optimization process, surpassing the prediction accuracy reported in similar studies by Lee et al. (2024) [53]. The experimental values closely matching predicted responses (floating lag time: 64 vs 64.194 sec; drug release: 98.4 vs 98.333%) demonstrate the robustness of the QbD approach in developing gastroretentive formulations [54].

The in vitro release studies revealed systematic relationships between formulation composition and drug release patterns. The influence of HPMC K15M concentration on release profiles (Fig. 6) demonstrated a clear polymer-dependent control mechanism, with higher concentrations (250 mg) providing more sustained release (82.6—87.2% at 12 hours) compared to lower concentrations (150 mg, 94.8—98.4% at 12 hours). This relationship aligns with findings reported by Das et al. (2021) [55], where HPMC K15M above 200 mg significantly retarded drug release in floating matrices. The optimized formulation RF3 achieved an ideal release profile with initial burst release (28.4% at 1hour) followed by controlled release, similar to successful gastroretentive formulations reported in the literature [56]. The release kinetics analysis (Fig. 7) revealed Higuchi

model dominance (R^2 = 0.9975) with non-Fickian transport (n = 0.75), indicating a complex release mechanism involving both diffusion and polymer relaxation, consistent with previous studies on HPMC-based systems [57].

The comparative dissolution study (Fig. 8) demonstrated the superior controlled release properties of the optimized formulation in comparison to the traditional marketed product. The significant reduction in initial drug release (28.4% vs 45.6% at 1hour) and extended-release duration (12 hours vs 6 hours) achieved by formulation RF3 represents a substantial improvement over immediate- release tablets, comparable to enhancements reported by Nigusse et al. (2021) [58] for other gastroretentive systems. The release kinetics data, showing combined diffusion and erosion mechanisms, supports the robustness of the formulation design [59]. The sustained release pattern achieved through optimal polymer-gas generating agent combination offers potential advantages in terms of reduced dosing frequency and improved therapeutic efficiency, as suggested by previous clinical studies with gastroretentive formulations [60].

The accelerated stability studies of the optimized formulation demonstrated robust physicochemical stability and consistent performance characteristics over the 6-month testing period (Table 9). The minimal variations in physical parameters, including tablet weight (450.2 ± 2.1 to 450.8 ± 2.5 mg) and hardness (5.3 ± 0.3 to 5.1 ± 0.4 kp), align with findings reported by Xi et al. (2021) [61] for HPMC-based floating tablets stored under similar conditions. The stability of drug content (98.86% to 98.24%) with less than 1% degradation exceeds ICH guidelines for shelf-life prediction [62] and compares favourably with stability data reported for other gastroretentive formulations [63]. The preservation of physical appearance and mechanical properties suggests effective protection against moisture-induced changes, a critical concern highlighted in previous stability studies of floating tablets [64]. While the in vitro results are promising, animal model evaluation is crucial to validate gastric retention behaviour, assess bioavailability enhancement, and establish in vitro—in vivo correlation (IVIVC). Pharmacokinetic studies in suitable animal models should demonstrate sustained plasma levels and reduced fluctuations compared to immediate-release formulations.

Several unexpected observations warrant discussion. The near-perfect drug content uniformity (96.72—98.65%) across all formulations may indicate either excellent manufacturing consistency or insufficient sensitivity in analytical methods. The remarkably consistent floating behaviour with minimal variability suggests possible idealized conditions that may not reflect real-world manufacturing variations. The rapid achievement of optimization with high desirability values (0.847) within a limited experimental space raises questions about the comprehensiveness of the design space exploration. Furthermore, the stability data showing minimal functional property changes over 6 months under stress conditions appears optimistic compared to typical pharmaceutical formulations and requires validation through independent studies.

The maintenance of functional properties, particularly floating characteristics and drug release profile, provides strong evidence for formulation stability. The marginal increase in floating lag time (64 to 69 seconds) and slight decrease in floating duration (11.4 to 11.0 hours) remain within acceptable limits for gastroretentive systems. The consistent drug release profile (98.4% to 97.4% at 12 hours) with minimal variation suggests stable matrix integrity and drug release mechanisms, comparable to stability results reported by Bachhav et al. (2024) for similar controlled release formulations. The overall stability profile indicates that the formulation would maintain its critical quality attributes under normal storage conditions, with projected stability exceeding 24 months based on accelerated testing guidelines [66], supporting its potential for commercial development.

While the current study demonstrates promising in vitro characteristics, several challenges remain unaddressed. The economic feasibility of this formulation compared to conventional tablets, scalability concerns for large-scale manufacturing, and regulatory approval pathways for gastroretentive systems in leprosy treatment require careful consideration. The clinical significance of 12 hours' sustained release versus traditional dosing regimens needs validation through pharmacokinetic and efficacy studies.

Several limitations must be acknowledged in this study. The relatively small sample size (n = 3) for each parameter may not fully represent batch-to-batch variability in commercial production. The dissolution studies were conducted only in 0.1 N HCl, which may not reflect the complex gastric environment with varying pH, enzymes, and food effects. The stability study period of 6 months under accelerated conditions provides limited insight into long-term storage behaviour, and the observed degradation patterns warrant further investigation. Additionally, the floating characteristics were evaluated under simplified in vitro conditions that may not accurately predict in vivo gastric retention behaviour. The lack of bioavailability studies limits the translation of these findings to clinical efficacy.

5. Conclusion

The present research established and characterized a floating gastroretentive tablet of dapsone using a Quality by Design approach. Comparing the results, it was seen that the optimized formulation (RF3) containing 150 mg HPMC K15M and 25 mg $NaHCO_3$ exhibited good floating characteristics with a lag time of 64 sec and a floatation duration of 11.4 hours for the said formulation, and exhibited a good percentage drug release of 98.4 % over 12 hours. In accelerated tests, the formulation maintained its stability with less than 6 months' variation in critical quality attributes. The mechanism of release kinetics aligned with the Higuchi model (R^2 = 0.9975), suggesting a non-Fickian release, depicting controlled release of the drug. The new formulation presents potential benefits over conventional tablets in terms of reduced dosing frequency and sustained drug release, which may theoretically improve patient compliance, though clinical validation is required to confirm therapeutic benefits. However, comprehensive in vivo studies are essential to validate this gastroretentive system. Animal model studies should evaluate gastric retention time, pharmacokinetic parameters, and bioavailability compared to conventional tablets. Subsequently, clinical trials are required to confirm therapeutic efficacy, safety, and patient compliance improvements in leprosy treatment before clinical implementation.

Abbreviations: ANOVA: Analysis of Variance; API: Active Pharmaceutical Ingredient; DSC: Differential Scanning Calorimetry; DoE: Design of Experiments; FTIR: Fourier-transform Infrared Spectroscopy; GRDDS: Gastroretentive Drug Delivery System; HPMC: Hydroxypropyl Methylcellulose; ICH: International Conference on Harmonisation; MCC: Microcrystalline Cellulose; MDT: Multi-drug Therapy; $NaHCO_3$: Sodium Bicarbonate; PVP: Polyvinylpyrrolidone; QbD: Quality by Design; RH: Relative Humidity; RPM: Rotations Per Minute; SD: Standard Deviation; UV: Ultra-violet Spectroscopy; USP: United States Pharmacopeia; WHO: World Health Organization; 2FI: Two-Factor Interaction.

Acknowledgements: The writers are grateful to Principal of the Institute for his assistance and direction during the study process. Completing this research was made possible by his invaluable advice and unwavering support. The gift sample of Dapsone that was provided by Sciquaint Innovations (OPC) Private Limited, Pune, India, is also appreciated by the authors for helping to conduct this research.

Author Contributions: Conceptualization – R. Mahale; Methodology – R. Mahale, S. Jadhav; Validation – R. Mahale, S. Jadhav, S. Mahajan; Formal Analysis – R. Mahale; Investigation – R. Mahale; Resources – R. Mahale; Data Curation – R. Mahale; Writing – Original Draft Preparation – R. Mahale; Writing – Review & Editing – R. Mahale, S. Jadhav; Visualization – R. Mahale; Supervision – S. Mahajan; Project Administration – S. Jadhav.

Funding: This research received no external funding.

Conflicts of Interest: The authors declare no conflict of interest.

References:

1. World Health Organization. Interruption of Transmission and Elimination of Leprosy Disease: Technical Guidance. Available online: https://www.who.int (Last accessed on 8 May 2025).
2. Chen, Y.Z.; Li, W.H.; Wu, Q.; Liu, Y.; Wang, X.M.; Xu, Y.Y.; et al. Evaluation of the economic burden of leprosy among migrant and resident patients in Guangdong Province, China. *BMC Infect. Dis.* **2017**, *17*, Art. No: 760. DOI: 10.1186/s12879-017-2869-8
3. Temiz, S.A.; Daye, M. Dapsone for the treatment of acne vulgaris: Do the risks outweigh the benefits? *Cutan. Ocul. Toxicol.* **2022**, *41*, 60–66. DOI: 10.1080/15569527.2021.2024565
4. Platsidaki, E.; Kontochristopoulos, G. Dapsone. In *European Handbook of Dermatological Treatments*; Katsambas, A.D., Lotti, T.M., Dessinioti, C., D'Erme, A.M., Eds.; Springer: Cham, Switzerland, **2023**; pp. 1645–1651. DOI: 10.1007/978-3-031-15130-9-145.
5. Khalilzadeh, M.; Shayan, M.; Jourian, S.; Rahimi, M.; Sheibani, M.; Dehpour, A.R. A comprehensive insight into the anti-inflammatory properties of dapsone. *Naunyn Schmiedebergs Arch. Pharmacol.* **2022**, *395*, 1509–1523. DOI: 10.1007/s00210-022-02297-1
6. Chaudhari, K.D.; Nimbalwar, M.G.; Singhal, N.S.; Panchale, W.A.; Manwar, J.V.; Bakal, R.L. Comprehensive review on characterizations and application of gastro-retentive floating drug delivery system. *GSC Adv. Res. Rev.* **2021**, *7*, 35–44. DOI: 10.30574/gscarr.2021.7.1.0070
7. Mora-Castaño, G.; Domínguez-Robles, J.; Himawan, A.; Millán-Jiménez, M.; Caraballo, I. Current trends in 3D printed gastroretentive floating drug delivery systems: A comprehensive review. *Int. J. Pharm.* **2024**, *663*, Art. No. 124543. DOI: 10.1016/j.ijpharm.2024.124543
8. Vinchurkar, K.; Sainy, J.; Khan, M.A.; Sheetal, M.; Mishra, D.K.; Dixit, P. Features and facts of a gastroretentive drug delivery system: A review. *Turk. J. Pharm. Sci.* **2022**, *19*, 476–483. DOI: 10.4274/tjps.galenos.2021.44959
9. Attimarad, M.; Nair, A.B.; Sreeharsha, N.; Al-Dhubiab, B.E.; Venugopala, K.N.; Shinu, P. Development and validation of green UV derivative spectrophotometric methods for simultaneous determination of metformin and remogliflozin. *Int. J. Environ. Res. Public Health* **2021**, *18*, Art. No. 448. DOI: 10.3390/ijerph18020448
10. Alburyhi, M.M.; Hamidaddin, M.A.; Noman, M.A.; Saif, A.A.; Yahya, T.A.; Al-Ghorafi, M.A. Rivaroxaban-excipient compatibility studies for advanced drug delivery systems development. *Eur. J. Pharm. Med. Res.* **2024**, *11*, 370–404.
11. Alburyhi, M.M.; Noman, M.A.; Saif, A.A.; Al-Ghorafi, M.A.; Yahya, T.A.; Yassin, S.H.; et al. Diclofenac-excipient compatibility studies for advanced drug delivery systems development. *World J. Pharm. Res.* **2024**, *13*, 1297–1333. DOI: 10.20959/wjpr202414-33329
12. Kuril, A.K. Differential scanning calorimetry: A powerful and versatile tool for analyzing proteins and peptides. *J. Pharm. Res. Int.* **2024**, *36*, 179–187. DOI: 10.9734/jpri/2024/v36i77549
13. Fatahi, H.; Claverie, J.; Poncet, S. Thermal characterization of phase change materials by differential scanning calorimetry: A review. *Appl. Sci.* **2022**, *12*, Art. No. 12019. DOI: 10.3390/app122312019
14. Parmar, S.; Patel, J.; Patel, N.; Patel, A. Formulation development, optimization and in vitro evaluation of gas-based gastroretentive drug delivery system of anti-diabetic drug. *World J. Pharm. Sci.* **2022**, *10*, 64–83. DOI: 10.54037/WJPS.2022.100607
15. Pandey, S.K.; Pudasaini, J.; Parajuli, N.; Singh, R.E.; Shah, K.P.; Adhikari, A.; et al. Formulation and evaluation of floating tablet of nimesulide by direct compression method. *Magna Sci. Adv. Res. Rev.* **2024**, *10*, 153–161. DOI: 10.30574/msarr.2024.10.1.0008
16. Chitte, N.; Jadhav, S.; Shinde, S.; Deshmukh, A.; Patil, C. Formulation and evaluation of gastroretentive floating beads of valsartan. *Cuest. Fisioter.* **2025**, *54*, 1813–1832.
17. Gopaiah, K.V.; Kumar, J.N.; Teja, M.R.; Lokesh, T.; Sruthi, D.S.; Roja, M.; et al. Development and assessment of hydroxypropyl methylcellulose-based floating tablets for ciprofloxacin HCL using direct compression technique. *J. Pharm. Res.* Int. **2024**, *36*, 47–62. DOI: 10.9734/jpri/2024/v36i37506
18. Kunnath, K.; Chen, L.; Zheng, K.; Davé, R.N. Assessing predictability of packing porosity and bulk density enhancements after dry coating of pharmaceutical powders. *Powder Technol.* **2021**, *377*, 709–722. DOI: 10.1016/j.powtec.2020.09.037

19. Kalman, H. Bulk densities and flowability of non-spherical particles with mono-sized and particle size distributions. *Powder Technol*. **2022**, *401*, Art. No. 117305. DOI: 10.1016/j.powtec.2022.117305.

20. Schlick-Hasper, E.; Bethke, J.; Vogler, N.; Goedecke, T. Flow properties of powdery or granular filling substances of dangerous goods packagings. *Packag. Technol. Sci.* **2022**, *35*, 765–782. DOI: 10.1002/pts.2678

21. Kaleem, M.A.; Alam, M.Z.; Khan, M.; Jaffery, S.H.I.; Rashid, B. Experimental investigation on accuracy of Hausner ratio and Carr index of powders. *Met. Powder Rep.* **2021**, *76*, S50–S54. DOI: 10.1016/j.mprp.2020.06.061

22. Jadhav, S.P.; Ahire, S.M.; Shewale, V.V.; Patil, C.D.; Pagar, R.Y.; Sonawane, D.D.; et al. Formulation of tablet of nifedipine co-crystal for enhancement of solubility. *Biosci. Biotechnol. Res. Asia* **2025**, *22*, 191–200. DOI: 10.13005/bbra/3353

23. Ansari, M.H. Preclinical drug development process: Formulation and development aspects. *Int. J. Med. Phar. Sci.* **2023**, *13*, Art. No. 1. DOI: 10.31782/IJMPS.2023.13301

24. Asrade, B.; Tessema, E.; Tarekegn, A. In vitro comparative quality evaluation of different brands of carbamazepine tablets. *BMC Pharmacol. Toxicol.* **2023**, *24*, Art. No. 35. DOI: 10.1186/s40360-023-00670-1

25. Ukwueze, S.E.; Jonathan, C.I.; Ezeh, I.N.; Oti, I.E.; Chukwu, D.E.; Chukwuogor, C.; et al. Formulation and evaluation of diazepam tablet from solidified self-emulsifying drug delivery system. *World J. Pharm. Sci.* **2021**, *9*, 150–161. DOI: 10.54037/WJPS.2021.91206

26. Vetrivel, D.; Ilango, K.B.; Bhuvaneswari, S.; Gomathi, P.; Kowsalya Devi, M. In-vitro comparative study of generic vs branded tablets–A review. *World J. Pharm. Res.* **2023**, *12*, 419–437. DOI: 10.20959/wjpr202322-30569

27. Sharma, S.; Gupta, S.; Bhardwaj, B.; Sahu, A. A comparative analysis of metformin hydrochloride tablets, both branded and generic. *Int. J. Pharm. Sci. Rev. Res.* **2023**, *16*, 4207–4221.

28. Shimu, S.A. *Comparative Evaluation of Atorvastatin 20 mg Tablets Marketed in Bangladesh*. Bachelor of Pharmacy Thesis, Brac University, Dhaka, Bangladesh, September **2024**.

29. Islam, M.R.; Hossain, M.S.; Hossain, M.S.; Islam, M.T.; Sultana, S.; Nijhum, N.; et al. Quality assessment of hydroxychloroquine tablet. *Prog. Microbes Mol. Biol.* 2023, *6*, Art. No. a0000336. DOI: 10.36877/pmmb.a0000336

30. Jadhav, S.P.; Patil, D.M.; Sonawane, D.D.; Patil, P.D.; Ghugarkar, P.G.; Saad, M. Formulation of tablet of ivermectin co-crystal. *J. Pharm. Negat. Results* **2023**, *14*, 513–520. DOI: 10.47750/pnr.2023.14.S01.60

31. Won, D.H.; Park, H.; Ha, E.S.; Kim, H.H.; Jang, S.W.; Kim, M.S. Optimization of bilayer tablet manufacturing process. *Int. J. Pharm.* **2021**, *605*, Art. No. 120838. DOI: 10.1016/j.ijpharm.2021.120838

32. Sanoj, R.; Sunny, S.S.; Mohasin, S.; Jeffisha, F. Innovations in drug release: A review on gastroretentive drug delivery systems. *IJPPR.Human* **2023**, *28*, 104–123.

33. Kumar, A.; Srivastava, R. In vitro in vivo studies on floating microspheres. *Asian J. Pharm. Clin. Res.* **2021**, *14*, 13–26. DOI: 10.22159/ajpcr.2021.v14i1.39183

34. Ranjan, A.; Jha, P.K. Studying drug release through polymeric controlled release formulations. *Mol. Pharm.* **2021**, *18*, 2600–2611. DOI: 10.1021/acs.molpharmaceut.1c00086

35. Javed, Q.U.A.; Syed, M.A.; Arshad, R.; Rahdar, A.; Irfan, M.; Raza, S.A.; et al. Prolonged release mucoadhesive tablets of dexamethasone. *Pharmaceutics* **2022**, *14*, Art. No. 807. DOI: 10.3390/pharmaceutics14040807

36. González-González, O.; Ramirez, I.O.; Ramirez, B.I.; O'Connell, P.; Ballesteros, M.P.; Torrado, J.J. Drug stability: ICH versus accelerated predictive stability studies. *Pharmaceutics* **2022**, *14*, Art. No. 2324. DOI: 10.3390/pharmaceutics14112324

37. Henninger, B.; Plaikner, M.; Zoller, H.; Viveiros, A.; Kannengiesser, S.; Jaschke, W.; et al. Performance of Dixon-based methods for MR liver iron assessment. *Eur. Radiol.* **2021**, *31*, 2252–2262. DOI: 10.1007/s00330-020-07291-w

38. Scrivens, G. Theory and fundamentals of accelerated predictive stability (APS) studies. In *Accelerated Predictive Stability*; Gerst, P., Ed.; Elsevier: Amsterdam, The Netherlands, **2018**; pp. 39–65.

39. Zhou, W.; He, Y.; Liu, F.; Liao, L.; Huang, X.; Li, R.; et al. Carboxymethyl chitosan–pullulan edible films enriched with galangal essential oil. *Carbohydr. Polym.* **2021**, *256*, Art. No. 117579. DOI: 10.1016/j.carbpol.2020.117579

40. Aminu, N.; Chan, S.Y.; Mumuni, M.A.; Umar, N.M.; Tanko, N.; Zauro, S.A.; et al. Physicochemical compatibility studies of triclosan and flurbiprofen. *Future J. Pharm. Sci.* **2021**, *7*, Art. No. 148. DOI: 10.1186/s43094-021-00302-7

41. Diño, S.F.; Edu, A.D.; Francisco, R.G.; Gutierrez, E.; Crucis, P.; Lapuz, A.M.; et al. Drug-excipient compatibility testing of cilostazol. *Philipp. J.* **Sci**. **2023**, *152*, 2129–2137. DOI: 10.56899/152.6A.08

42. Almotairi, N.; Mahrous, G.M.; Al-Suwayeh, S.; Kazi, M. Design and optimization of lornoxicam dispersible tablets. *Pharmaceuticals* **2022**, *15*, Art. No. 1463. DOI: 10.3390/ph15121463

43. Bhatia, V.; Dhingra, A.K.; Dass, R.; Chopra, B.; Guarve, K. Formulation and development of escitalopram fast dissolving tablets. *Cent. Nerv. Syst. Agents Med. Chem.* **2022**, *22*, 198–213. DOI: 10.2174/1871524922666220624113719

44. Al Hablawi, M.F.; Jaffar, I.S. Formulation variables influencing ketoconazole gastroretentive drug delivery system. *Al-Rafidain J. Med. Sci.* **2024**, *7*, S15–S23. DOI: 10.54133/ajms.v7i1.867

45. Su'udiyah, U.F.; Sugiyartono. Effect of ethyl cellulose on floating characteristic and ranitidine HCL release from floating tablet. *Res. J. Pharm. Technol.* **2021**, *14*, 735–740. DOI: 10.5958/0974-360X.2021.00128.1

46. Jaimini, R.; Jaimini, M. Formulation and optimization of gastro-retentive floating tablets of enalapril maleate and losartan. *Trop. J. Pharm. Life Sci.* **2025**, *12*, 01–10. DOI: 10.61280/tjpls.v12i1.170

47. Moravkar, K.K.; Shah, D.S.; Magar, A.G.; Bhairav, B.A.; Korde, S.D.; Ranch, K.M.; et al. Assessment of pharmaceutical powders flowability. J. *Drug Deliv. Sci. Technol.* **2022**, *71*, Art. No. 103265. DOI: 10.1016/j.jddst.2022.103265

48. Patel, M.; Shelke, S.; Surti, N.; Panzade, P.; Al-Keridis, L.A.; Upadhyay, T.K.; et al. Design, preparation, and in vitro evaluation of gastroretentive floating matrix tablet of mitiglinide. *Front. Pharmacol.* **2023**, *14*, Art. No. 1140351. DOI: 10.3389/fphar.2023.1140351

49. Syed, S.M.; Gawale, K.; Farooqui, Z.S. Formulation development and evaluation of gastro retentive matrix tablet of levamisole hydrochloride. *Pharm. Biosci. J.* **2021**, *9*, 50–70. DOI: 10.20510/ukjpb/9/i1/1611533539

50. Indurkhya, A.; Masheer, K.A. Box–Behnken design for optimization of formulation variables for controlled release gastroretentive tablet of verapamil hydrochloride. *Int. J. Appl. Pharm.* **2023**, *15*, 256–263. DOI: 10.22159/ijap.2023v15i1.46489

51. Patel, M.B.; Shaikh, F.; Patel, V.B.; Surti, N. Application of experiential design for framing gastroretentive microsponges of glipizide. *Indian J. Pharm. Educ. Res.* **2021**, *55*, 966–978. DOI: 10.5530/ijper.55.4.197

52. Patel, A.; Modasiya, M.; Shah, D.; Patel, V. Development and in vivo floating behavior of verapamil HCl intragastric floating tablets. *AAPS PharmSciTech* **2009**, *10*, 310–315. DOI: 10.1208/s12249-009-9210-9

53. Lee, Y.S.; Kang, J.S.; Kim, K.M.; Pyo, J.S. Optimization of ticagrelor tablet for gastro-retentive drug delivery using full factorial design. *Trop. J. Pharm. Res.* 2024, *23*, 235–242. DOI: 10.4314/tjpr.v23i2.1

54. Jadhav, S.P.; Patil, D.M.; Sonawane, D.D.; Gaikwad, V.B.; Patil, P.D.; Ghugarkar, P.G. Formulation development and evaluation of orally disintegrating tablet of clopidogrel bisulphate. *Int. J. Res. Pharm. Sci.* **2023**, *14*, 505–512. DOI: 10.26452/ijrps.v14i1.5206

55. Das, S.; Kaur, S.; Rai, V.K. Gastro-retentive drug delivery systems: A recent update on clinical pertinence and drug delivery. *Drug Deliv. Transl. Res.* **2021**, *11*, 1849–1857. DOI: 10.1007/s13346-020-00875-5

56. Raja, H.N.; Din, F.U.; Shabbir, K.; Khan, S.; Alamri, A.H.; Al Awadh, A.A.; et al. Sodium alginate-based smart gastro-retentive drug delivery system of revaprazan loaded SLNs. *Int. J. Biol. Macromol.* **2023**, *253*, Art. No. 127402. DOI: 10.1016/j.ijbiomac.2023.127402

57. Mir, A.; Kumar, A.; Alam, J.; Riaz, U. Synthesis and characterization of pH-responsive composite hydrogels for sustained release of amoxicillin drug. *Int. J. Biol. Macromol.* **2023**, *252*, Art. No. 126015. DOI: 10.1016/j.ijbiomac.2023.126015

58. Nigusse, B.; Gebre-Mariam, T.; Belete, A. Design, development and optimization of sustained release floating, bioadhesive and swellable matrix tablet of ranitidine hydrochloride. *PLoS ONE* **2021**, *16*, Art. No. e0253391. DOI: 10.1371/journal.pone.0253391

59. Sousa, A.S.; Serra, J.; Estevens, C.; Costa, R.; Ribeiro, A.J. Unveiling swelling and erosion dynamics of mirabegron extended release tablets. *AAPS PharmSciTech* **2024**, *25*, Art. No. 277. DOI: 10.1208/s12249-024-02994-5.

60. Elkomy, M.H.; Abou-Taleb, H.A.; Eid, H.M.; Yassin, H.A. Fabrication and in vitro/in vivo appraisal of metronidazole intra-gastric buoyant sustained-release tablets. *Pharmaceutics* **2022**, *14*, Art. No. 863. DOI: 10.3390/pharmaceutics14040863

61. Xi, Z. *QBD Approach for Development of Ivermectin-Loaded Gastro-Retentive Sustained Release Tablets as Mass Drug Administration for Malaria Transmission Control*. Ph.D. Dissertation, Saint John's University, Jamaica, New York, USA, **2021**.

62. Gaikwad, D.T.; Patil, S.J.; Killedar, S.G.; Wadkar, G.H.; Mali, D.P.; Jadhav, S.A. Formulation and evaluation of domperidone maleate mucoadhesive system using *Cassia fistula* L. seed mucilage. *J. Med. Pharm. Allied Sci.* **2022**, *11*, 5318–5324. DOI: 10.55522/jmpas.V11I5.4203

63. Yoshida, T.; Kojima, H. Oral drug delivery systems applied to launched products: Value for the patients and industrial considerations. *Mol. Pharm.* **2023**, *20*, 5312–5331. DOI: 10.1021/acs.molpharmaceut.3c00482

64. Kim, D.H.; Lee, S.W.; Lee, J.H.; Park, J.W.; Park, S.M.; Maeng, H.J.; et al. Development of gastroretentive floating combination tablets containing amoxicillin trihydrate and levofloxacin. *Pharmaceutics* **2024**, *16*, Art. No. 1242. DOI: 10.3390/pharmaceutics16101242